RESEARCH ARTICLE

AMERICAN JOURNAL OF medical genetics PART A

Characterization of X-linked Hypohidrotic Ectodermal Dysplasia (XL-HED) Hair and Sweat Gland Phenotypes Using Phototrichogram Analysis and Live Confocal Imaging

Kyle B. Jones,[1†] Alice F. Goodwin,[1†] Maya Landan,[1] Kerstin Seidel,[1] Dong-Kha Tran,[1] Jacob Hogue,[2] Miquella Chavez,[1] Mary Fete,[3] Wenli Yu,[1] Tarek Hussein,[1] Ramsey Johnson,[4] Kenneth Huttner,[4] Andrew H. Jheon,[1] and Ophir D. Klein[1,2,5*]

[1]Program in Craniofacial and Mesenchymal Biology, University of California, San Francisco, San Francisco, California

[2]Division of Medical Genetics, Department of Pediatrics, University of California, San Francisco, San Francisco, California

[3]National Foundation for Ectodermal Dysplasias, Mascoutah, Illinois

[4]Edimer Pharmaceuticals, Inc., Cambridge, Massachusetts

[5]Center for Craniofacial Anomalies, Department of Orofacial Sciences, University of California, San Francisco, San Francisco, California

Manuscript Received: 7 December 2012; Manuscript Accepted: 9 February 2013

Hypohidrotic ectodermal dysplasia (HED) is the most common type of ectodermal dysplasia (ED), which encompasses a large group of syndromes that share several phenotypic features such as missing or malformed ectodermal structures, including skin, hair, sweat glands, and teeth. X-linked hypohidrotic ectodermal dysplasia (XL-HED) is associated with mutations in ectodysplasin (*EDA1*). Hypohidrosis due to hypoplastic sweat glands and thin, sparse hair are phenotypic features that significantly affect the daily lives of XL-HED individuals and therefore require systematic analysis. We sought to determine the quality of life of individuals with XL-HED and to quantify sweat duct and hair phenotypes using confocal imaging, pilocarpine iontophoresis, and phototrichogram analysis. Using these highly sensitive and non-invasive techniques, we demonstrated that 11/12 XL-HED individuals presented with a complete absence of sweat ducts and that none produced sweat. We determined that the thin hair phenotype observed in XL-HED was due to multiple factors, such as fewer terminal hairs with decreased thickness and slower growth rate, as well as fewer follicular units and fewer hairs per unit. The precise characterization of XL-HED phenotypes using sensitive and non-invasive techniques presented in our study will improve upon larger genotype–phenotype studies and the assessment of future therapies in XL-HED.

Key words: X-linked hypohidrotic ectodermal dysplasia; ectodysplasin; hair; sweat gland; terminal hair; confocal imaging; pilocarpine iontophoresis; phototrichogram

How to Cite this Article:
Jones KB, Goodwin AF, Landan M, Seidel K, Tran D-K, Hogue J, Chavez M, Fete M, Yu W, Hussein T, Johnson R, Huttner K, Jheon AH, Klein OD. 2013. Characterization of X-linked hypohidrotic ectodermal dysplasia (XL-HED) hair and sweat gland phenotypes using phototrichogram analysis and live confocal imaging.
Am J Med Genet Part A 161A:1585–1593.

INTRODUCTION

Ectodermal dysplasia (ED) describes a large group of syndromes characterized by missing or malformed ectodermal structures,

Additional supporting information may be found in the online version of this article.

[†]Kyle B. Jones and Alice F. Goodwin contributed equally to this work.

Conflict of interest: Edimer Pharmaceuticals provided funding for the study as well as technical assistance. The academic authors independently analyzed all data. Additionally, the decision about where and what to publish was decided solely by the first and corresponding authors.

Grant sponsor: National Institutes of Health; Grant numbers: F30-DE022509; F30-DE022205; K99-DE022059; R01-DE021420; Grant sponsor: Edimer Pharmaceuticals.

[*]Correspondence to:
Ophir D. Klein, University of California, San Francisco, 513 Parnassus Ave, HSE1509, San Francisco, CA 94143.
E-mail: ophir.klein@ucsf.edu

Article first published online in Wiley Online Library (wileyonlinelibrary.com): 17 May 2013
DOI 10.1002/ajmg.a.35959

including skin, hair, sweat glands, and teeth [reviewed in Mikkola, 2009]. Hypohidrotic ectodermal dysplasia (HED) is the most prevalent type of ED and is inherited in an X-linked (XL), autosomal recessive (AR), or autosomal dominant (AD) manner. The incidence of XL-HED is estimated at 1–10 in 100,000 live male births, and the carrier incidence is around 17.3 in 100,000 women [Mortier and Wackens, 2004; Nguyen-Nielsen et al., 2013]. The clinical features of XL-HED include severe hypohidrosis, sparse hair and eyebrows, periorbital wrinkling, dry skin, missing and malformed teeth, increased susceptibility to respiratory infections, as well as hypoplasia of sweat, sebaceous, meibomian, lacrimal, and mammary glands [Clarke et al., 1987; Clauss et al., 2008]. XL-HED is caused by mutations in the gene encoding ectodysplasin (*EDA1*), a ligand in the tumor necrosis factor (TNF) superfamily. AR-HED and AD-HED are caused by mutations in the EDA receptor (EDAR), or the cytosolic, EDAR-specific adaptor molecule called EDAR-associated death domain (EDARADD) [Mikkola and Thesleff, 2003].

A major cause of mortality and morbidity in infants with XL-HED is hyperthermia due to sweat gland hypoplasia and hypohidrosis. The mortality rate of XL-HED individuals in the first year of life is estimated to be 2.1% [Blüschke et al., 2010]. Additionally, the majority of XL-HED individuals experience fevers early in life. It has been suggested that acute episodes of severe hyperthermia, which can lead to febrile seizures, may be associated with developmental abnormalities [Blüschke et al., 2010]. Heat intolerance later in life continues to affect those with XL-HED, limiting their ability to perform many daily activities, especially exercise [Hammersen et al., 2011]. Sparse hair can also significantly impact XL-HED individuals beginning in young adulthood, due to its negative psychosocial consequences. Therefore, novel or improved therapies for sweat gland hypoplasia and sparse hair may dramatically improve the lives of XL-HED individuals.

A great deal is known about the role of the EDA pathway in ectoderm-derived tissue and organ development based on data from mice and humans. Mice with spontaneous mutations that phenocopy characteristics of HED were found to carry mutations in *Eda*, *Edar*, or *Edaradd* [Reviewed in Courtney et al., 2005]. *Eda*, *Edar*, and *Edaradd* are expressed in the epithelium of the skin and become restricted to the placode during development [Cui and Schlessinger, 2006]. The EDA pathway is activated in the ectoderm by inductive Wnt/βcatenin signals from the underlying mesenchyme [Zhang et al., 2009], and in turn, activates the NF-κB pathway and downstream targets including Shh, Wnt, and BMP. Interestingly, in humans, a non-synonymous single nucleotide polymorphism (SNP) in *EDAR* (1540T/C) common in East Asian populations enhances EDA signaling and contributes to the thick and straight hair phenotype, opposed to the thin, sparse hair observed in HED [Fujimoto et al., 2007; Mou et al., 2008].

Potential molecular therapies are in development to treat XL-HED patients, largely based on knowledge gained from studies in animal models. Pre- and perinatal treatment of mice carrying *Eda* mutations with recombinant human EDA1 alleviated many of the XL-HED-associated phenotypes involving hair, sweat glands, and teeth [Gaide and Schneider, 2003]. Indeed, a partial rescue of some hair types and molar morphology was possible when EDA1 was administered prior to birth, whereas sweat gland hypoplasia was rescued in the immediate postnatal period with EDA1 administration [Gaide and Schneider, 2003]. Thus, there appears to be a therapeutic window during which EDA1 administration is most effective. Furthermore, multiple characteristics of XL-HED were recognized in a German shepherd dog, including symmetrical hairlessness, missing and conical shaped teeth, an inability to sweat, and an increased rate of pulmonary infections. These features were later linked to a mutation in the canine *EDA* gene [Casal et al., 2005]. Most XL-HED dogs treated postnatally with recombinant human EDA1 developed a permanent dentition similar to controls, had significantly improved sweat response, and decreased incidence of respiratory infections. However, the hair phenotype was not rescued, likely because hair follicles in dogs normally form in utero prior to when EDA1 was administered [Casal et al., 2007; Mauldin et al., 2009]. Although EDA1 therapy did not fully rescue the dental, hair, and sweat phenotypes associated with XL-HED in the dog model, it did alleviate the morbidities associated with these phenotypes. These examples underscore the potentially significant therapeutic effects that EDA1 replacement therapy might have in the treatment of human XL-HED.

As progress is made towards initiating clinical trials to treat XL-HED subjects, it is critical that clinical features characterizing XL-HED phenotypes are more specifically defined. Quantitative, reproducible, and non-invasive methods to measure XL-HED phenotypes will enable researchers to accurately assess treatment efficacy. In this study, we analyzed and quantified sweat gland hypoplasia and sparse hair phenotypes using a novel application of confocal imaging, pilocarpine iontophoresis, and phototrichograms in a cohort of 12 XL-HED affected and 13 unaffected control males.

MATERIALS AND METHODS

Study Participant Recruitment and Demographics

This study was approved by the University of California, San Francisco Institutional Review Board. Primary objectives of the study were to quantitatively assess the number of palmar sweat ducts, sweat production, and hair characteristics. All study subjects, or their legal guardians if subjects were under 18 years of age, provided written informed consent prior to participation in the study. To participate in the study, subjects must never have used pharmacologic treatment for thinning hair and must have been at least 10 years of age. A total of 13 healthy male control subjects with no family history of XL-HED and 12 male case subjects previously diagnosed clinically with XL-HED participated in the study. XL-HED subjects were contacted from a list of patients seen at UCSF clinics or recruited at the National Foundation for Ectodermal Dysplasias (NFED) family conference. A convenience sample of control subjects was used; therefore, controls were not age or ethnicity matched with XL-HED subjects. The 12 XL-HED subjects consisted of two pairs of brothers and eight unrelated individuals representing 10 distinct families. Control subjects were all unrelated. The majority of subjects in both control and XL-HED cohorts were Caucasian (53.9% and 83.3%, respectively; Table I). The ages of the control cohort participants ranged from 19 to 29 years whereas the XL-HED cohort ages ranged from 11 to 29 years (Table I). The median age for both groups was approximately 25 years.

TABLE I. Demographic Characteristics of Control and XL-HED Subjects

	Control (N = 13)		XL-HED (N = 12)		*P*-value[a]
Demographic characteristic					
Age (in years, median [IQR])	25.5 (24.3–27.4)		25.5 (15.7–28.2)		0.51
Age range (in years)	19–29		11–29		
BMI (in kg/m^2, median [IQR])	23.7 (22.8–25.8)		21.7 (18.6–24.3)		0.10
Race	**n**	**%**	**n**	**%**	
Asian	3	23	0	0	
Black	0	0	1	8	
White	7	54	10	84	
Other	3	23	1	8	

[a]*P*-values were calculated using the Wilcoxon rank-sum test.

Medical Questionnaire

Participants were interviewed, and a detailed medical history was collected. The medical questionnaire, completed in part by control subjects and in total by XL-HED subjects, included questions pertaining to sweating, hair, skin, and quality of life (Table II).

Genotyping

Eleven of the affected subjects underwent genotyping for *EDA1* mutations to confirm a diagnosis of XL-HED. Previous genotyping for the *EDA1* gene confirmed a mutation at this locus for one subject (#23).

Pilocarpine-Induced Iontophoresis

Pilocarpine-induced iontophoresis was performed using the Wescor 3700 device (Wescor Biomedical Systems, Logan, UT). Two electrodes containing Pilogel Iontophoretic Discs (solid agar consisting of 96% water and 0.5% pilocarpine nitrate; Wescor) were placed on the forearms of study participants. 1.5 mA of current was run for 5 min through the electrodes, after which time they were removed, and a Macroduct Sweat Collector (Wescor) was placed over the site of pilocarpine iontophoresis. Sweat was collected for 30 min from a 57 mm^2 surface area. The maximum volume of sweat that can be collected with the Macroduct Sweat Collector is 93 μl, as estimated by weight.

Live Confocal Microscopy Imaging of Palmar Sweat Ducts

Sweat duct density (number/cm^2) in the thenar (thumb) region of the palm of each subject was determined through analysis of images collected by direct visualization with an FDA 510(k) device, the

TABLE II. Clinical Characteristics of XL-HED Subjects as Determined by Medical Questionnaire

	XL-HED (N = 12)		Controls (N = 13)	
Clinical characteristic	**n**	**%**	**n**	**%**
Heat intolerance	12	100	0	0
Exercise limited by heat intolerance	10	83	0	0
Decreased sweating	12	100	1	8
Unexplained fevers	2	17	0	0
Dry skin/eczema	12	100	n/a[a]	
Thinning hair and/or eyebrows	8	67	n/a	
Fingernails/toenails appear normal	9	75	n/a	
Chronic childhood nasal drainage/blockage	11	92	n/a	
Respiratory related problems as a child	8	67	n/a	
Asthma	5	42	n/a	
Dry mouth	7	58	n/a	
Dry eyes	5	42	n/a	
Hoarseness of voice	10	83	n/a	
Nose bleeds as a child	10	83	n/a	

[a]n/a, data not available. Control subjects not asked question on medical questionnaire.

Lucid VivaScope 1500 (www.lucid-tech.com). The Lucid VivaScope is a live confocal imaging device that enables live imaging of epithelial tissues and structures, including the visualization of sweat ducts [Rajadhyaksha et al., 1999]. The maximum depth of imaging is approximately 300 μm; however, in this study, images were taken at a depth of 20–40 μm above the base of the stratum corneum in order to visualize sweat ducts. An adhesive ring was placed on the subject's palm to which the VivaScope was attached via a magnetic lock. A series of photographs were taken of an area approximately 6 mm × 6 mm. An individual (R.J., included as an author) trained in the use of this device was involved in the acquisition of all images. Two independent observers blinded to subject XL-HED status quantified the sweat ducts in the images obtained by the VivaScope.

Phototrichogram Analysis

Total and anagen hair counts in the scalp were determined from color macrophotographs of clipped hair on the occipital scalp in a 1 cm^2 circular target area centered by a cosmetic ink dot, if necessary [Canfield, 1996; Van Neste et al., 2000]. Hair in the target area was clipped to approximately 1 mm for determination of preliminary total hair count and then clipped to the scalp to monitor hair growth over the 2–3 day period between visits. At Study Visit 2, a macrophotograph of the target area was taken for the determination of anagen and telogen hair counts, based on the number of hairs that had lengthened over the intervening time period. Macrophotographs were taken using a Nikon D90 digital camera at fixed focus, distance, and exposure with the use of a Nikon 60 mm lens and EpiFlash from Canfield Scientific, Inc. (Fairfield, NJ). All digital images were provided to Canfield Scientific, which served as the central photography reader for quality assurance and hair counting/analysis. Digital macrophotographs were analyzed by trained technicians who were blinded to subject XL-HED status. Hair analysis was performed by means of Canfield's proprietary computer-based imaging software. Study Visit 1 images were used to visually identify the number of follicular units as well as the number of vellus and terminally differentiated hairs that appeared to emerge from each follicular unit. If a hair shaft was obstructed by a gel bubble, tattoo ink, or other artifact, then the follicular unit was omitted from the analysis. Each follicular unit was manually tagged with parameters set for two hairs per unit, three hairs per unit, or four+ hairs per unit. Hair thickness and growth rate were also directly measured with the assistance of the analysis software. Alignment of images was possible for all subjects except subjects #11 (control) and #4 (XL-HED) because each had hair too light in color for optimal analysis. For this reason, subjects #11 and #4 were excluded from this analysis.

Statistical Methods

All statistical analyses were performed using Stata/SE 11.1 for Mac (StataCorp, College Station, TX). During data analysis, several variables did not follow normal distributions. For this reason, the more conservative non-parametric Wilcoxon Rank-Sum test was used to analyze all continuous data. Summary statistics for continuous variables are reported as the median and interquartile range (IQR). Categorical variables were analyzed using Fisher's Exact Test. Findings were considered statistically significant if $P < 0.05$.

RESULTS

Medical Questionnaire

Twelve XL-HED affected males and 13 unaffected control males between the ages of 11 and 29 were recruited for the study. Control subjects were asked a portion of questions on the medical questionnaire, while XL-HED subjects completed these along with additional questions pertaining to their condition. The data collected from the medical questionnaire are summarized in Table II. As previously reported, XL-HED subjects reported increased heat intolerance (12/12; $P < 0.0001$), limitations in exercise due to heat intolerance (10/12; $P < 0.0001$), and decreased sweating (12/12; $P < 0.0001$) compared with controls. Only 17% of XL-HED subjects reported experiencing unexplained fevers during childhood ($P = 0.22$), and no seizures were associated with these fevers. None in the control cohort reported any unexplained fevers.

The remainder of the medical history questionnaire information was obtained from XL-HED subjects only. XL-HED participants were presented with a list of lifestyle choices and asked to only select those choices affected by decreased sweating. The most common lifestyle choices affected by decreased sweating were involvement in outdoors sports (n = 11), daily life (n = 10), choice of occupation (n = 8), choice of vacation destination (n = 8), and decision to live in a cooler climate (n = 6). Of the 7/12 XL-HED subjects that reported suffering from dry mouth and the 5/12 from dry eyes, only four subjects reported suffering from both. Lastly, 10/12 subjects reported experiencing chronic nosebleeds as children, with most recalling onset of nosebleeds under the age of 5 (7/10). Eight of 10 subjects reported suffering from chronic nosebleeds as adults with a range of 3–75 nosebleeds per year.

Sweat Duct Counts

Live confocal microscopic imaging (Fig. 1a,b) revealed that control subjects had a median of 115 palmar sweat ducts per 36 mm^2 (intermediate quartile range [IQR]: 97.5–119.5), whereas XL-HED subjects had a median of 0 (IQR: 0–0; $P < 0.0001$; Fig. 1c). Interestingly, one of these XL-HED subjects (#8) presented with sweat ducts, but only half as many as the control subject with the fewest sweat ducts.

Pilocarpine-Induced Sweat Volumes

Using pilocarpine iontophoresis, control subjects had a median sweat volume of 52 μl (IQR: 33–63), whereas all XL-HED subjects produced no sweat (IQR: 0–0; $P < 0.0001$; Fig. 1d). One control subject (#16), whose sweat ducts were in the normal range and who did not report decreased sweating or heat intolerance, had pilocarpine-induced sweat volume that was minimal (i.e., 3 μl).

Hair Counts

In order to thoroughly characterize the hair phenotype in XL-HED subjects, various parameters of hair biology were analyzed. Human hair consists of two types, vellus and terminal hairs, that are

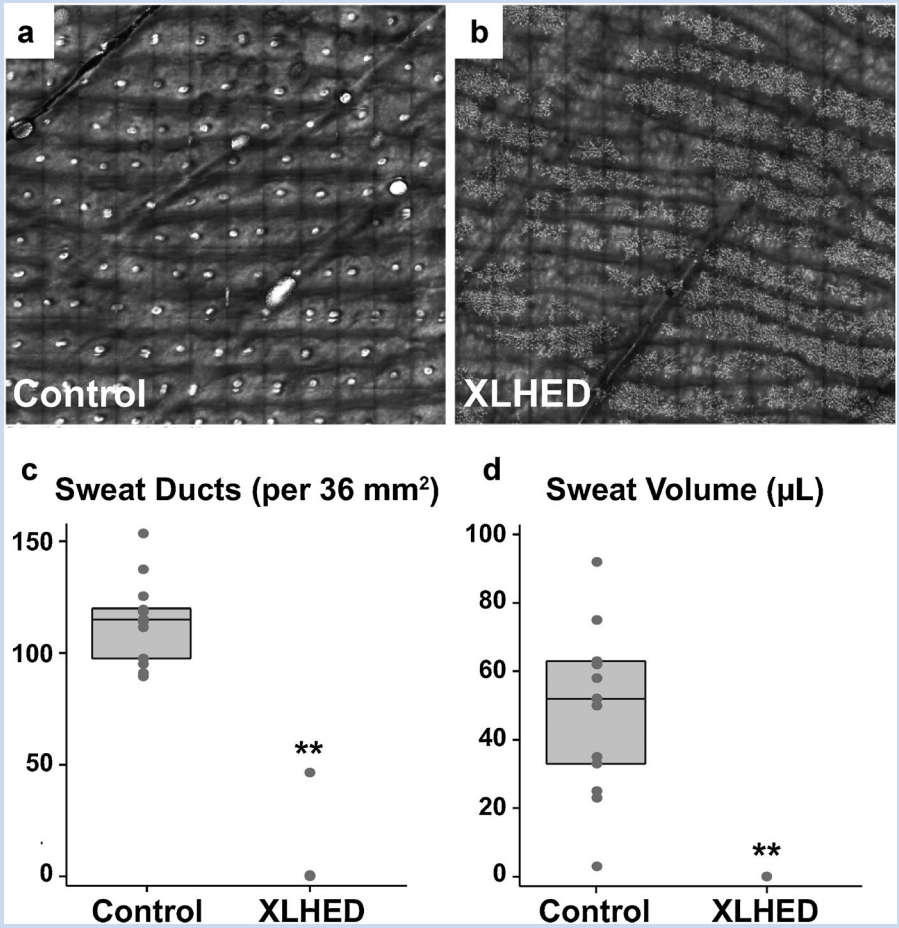

FIG. 1. XL-HED subjects show a decrease in palmar sweat ducts and produce little to no sweat. a,b: Live confocal imaging of a 36 mm^2 area of the palm shows an absence of sweat ducts in the XL-HED subject compared to control. Sweat ducts appear as small, round, white dots in the control subject. Note: spindly, white projections seen in the XL-HED subject (b) may be dendritic cells and were seen in both XL-HED and control subjects. c: Quantification of the number of palmar sweat ducts shows that XL-HED subjects have few sweat ducts compared to control subjects. d: Graph of the sweat volumes collected over 30 min using pilocarpine iontophoresis shows XL-HED subjects produced little to no sweat. Note that in (c) and (d), each circle corresponds to a measurement for an individual subject. The upper, middle, and lower horizontal lines in the rectangular box behind the circles represent the 75th, 50th (median), and 25th percentiles, respectively. $^{**}P < 0.0001$.

organized into follicular units (FUs). Vellus hairs are short, thin, and light in color whereas terminal hairs are long, thick, and often pigmented. Both vellus and terminal hair follicles repeatedly cycle through three distinct phases: anagen (growth), catagen (regression/involution of the hair), and telogen (resting phase). Vellus and terminal hairs differ in the cycling times for each phase (reviewed in [Stenn and Paus, 2001]). Since hair thickness correlates with the overall number of terminal hairs present, changes in the ratio of terminal to vellus hairs and/or the ratio of terminal anagen hairs to terminal telogen hairs are often associated with various hair pathologies, such as androgenetic alopecia (male and female pattern baldness) [Sinclair and Dawber, 2001].

All hair counts and subsequent hair analyses were calculated from a surface area of 1 cm^2 (Fig. 2a–d; eTable SI—see Supporting information online). Total hair counts were significantly different between groups, with control subjects having a median of 212 total hairs (IQR: 195.5–296.5) and XL-HED subjects having a median count of 93 (IQR: 80–134; $P = 0.0001$). Further analysis revealed that this large disparity was due primarily to a difference in terminal hair counts as opposed to vellus hairs. Control subjects had a median of 197.5 terminal hairs (IQR: 176.5–268) compared with XL-HED subjects that had a median of 84 terminal hairs (IQR: 64–97; $P < 0.0001$; Fig. 2e). Vellus hair counts were similar between control and XL-HED subjects. The ratio of terminal to vellus hairs in control subjects had a median ratio of 8.7 (IQR: 6.4–11.1), whereas XL-HED subjects had a median ratio of 3.2 (IQR: 2.4–14.5; $P = 0.30$). A terminal to vellus hair ratio of <4 typically denotes hair thinning [Sinclair and Dawber, 2001].

Follicular Units

XL-HED and control subjects differed significantly with respect to various FU characteristics (Fig. 2f). Controls presented with sig-

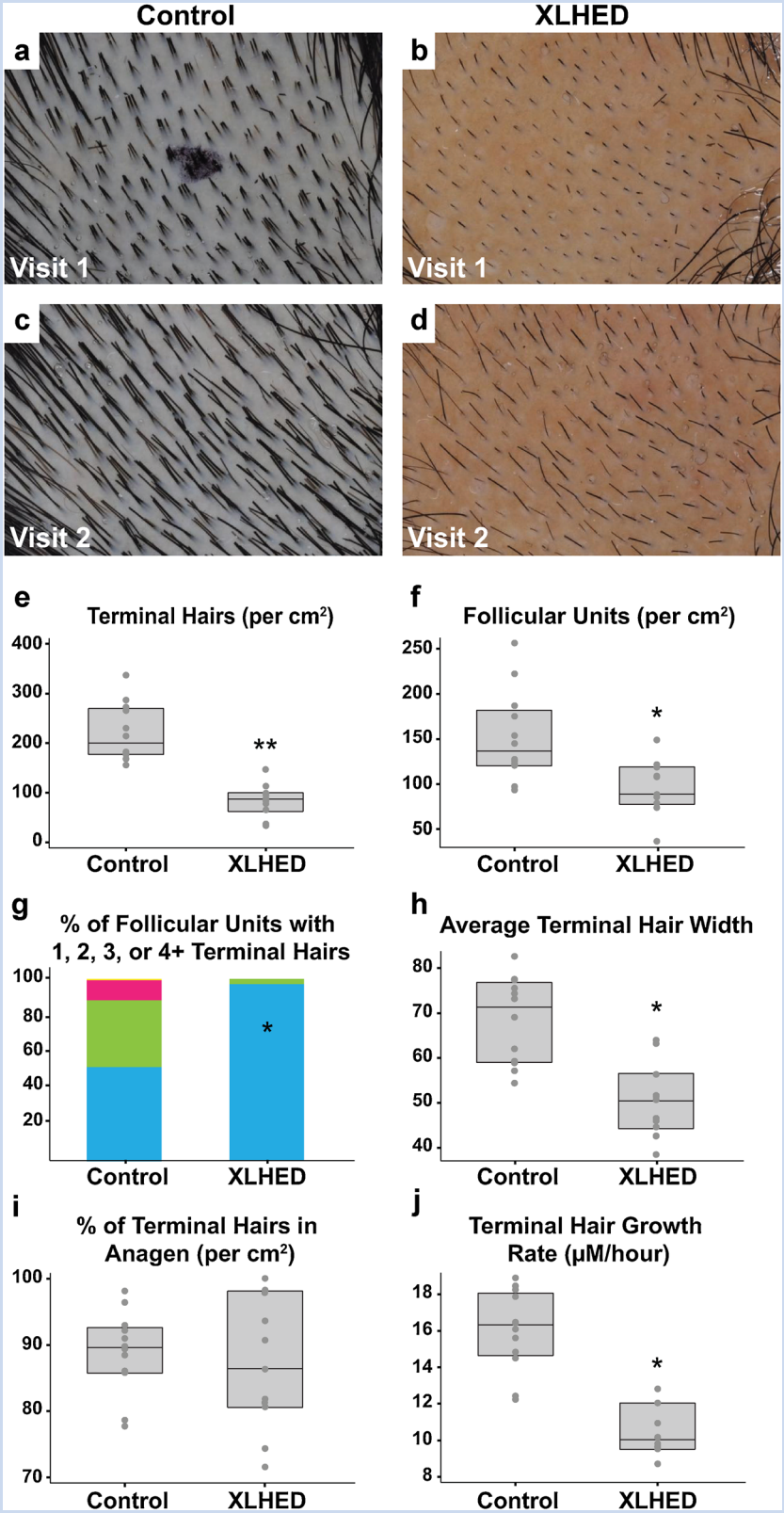

FIG. 2. Phototrichogram analysis reveals multiple properties of XL-HED subject hair that differ significantly from controls. a–d: Photographs of the shaved scalp in control and XL-HED subjects during study visit 1 (a,b) and again 2–3 days later (visit 2; c,d). Such images were utilized for phototrichogram analysis. Note: The small, circular black mark in (a) is a temporary ink tattoo used to help identify the subject's shaved area during study visit 2. In the control subject, the tattoo washed off by the time the second photograph was taken. e–j: Graphs representing measurements of various hair properties obtained after completion of the phototrichogram analysis in all study subjects. Note in (g), blue bar represents the % of follicular units with one hair, green is two hairs, pink is three hairs and yellow is four+ hairs. $^{*}P < 0.0005$; $^{**}P < 0.0001$.

nificantly more FUs per cm^2 with a median of 135.5 (IQR: 121–180.5) compared with XL-HED subjects who had a median of 88 FUs (IQR: 78–118; $P = 0.0021$; Fig. 2f). Controls also possessed a higher average number of hairs per FU with a median of 1.6 (IQR: 1.4–1.8), whereas XL-HED subjects had a median of 1 (IQR: 1–1.1; $P = 0.0003$).

We next analyzed the number of FUs in each group that had 1, 2, 3, and 4 or more hairs (FUs with more than four hairs were scarce, and it was difficult to determine the exact number of hairs present; thus, FUs with four or more hairs were grouped together). Since control subjects had significantly more FUs compared to XL-HED subjects, we calculated the percentages of FUs that had one, two, three, or four hairs. Strikingly, 97.2% (IQR: 90.6–100%) of FUs in XL-HED subjects had only one hair, whereas only 50.5% (IQR: 44.5–59.5%; $P < 0.0001$) of FUs in control subjects had one hair (Fig. 2g). There were also significant differences between control and XL-HED subjects in the number of FUs with two, three, and four or more hairs (Fig. 2g).

Hair Width

The width of terminal hairs in control subjects was significantly larger compared to XL-HED subjects. Controls had a median terminal hair width of 71 μm (IQR: 59–76.3), whereas XL-HED subjects had a median width of 50.5 μm (IQR: 44.5–56.2; $P = 0.0007$; Fig. 2h). There was no significant difference in the width of vellus hairs.

Hair Growth

We calculated the percent of terminal hairs that were in anagen (i.e., growth phase). Surprisingly, controls had a median of 89.5% of terminal hairs in anagen (IQR: 85.9–92.5%), and XL-HED subjects had a similar median of 86.3% (IQR: 80.5–97.9%; $P = 0.81$; Fig. 2i). The percentage of vellus hairs in anagen was also similar between groups ($P = 0.31$). Control subjects had faster growing terminal hairs with a median growth rate of 16.2 μm/hr (IQR: 14.6–18) compared with XL-HED subjects who had a median growth rate of 10.1 μm/hr (IQR: 9.6–12; $P = 0.0001$; Fig. 2j).

Genotyping of *EDA1*

Genotyping was performed on subjects (one per family) to confirm mutations in *EDA1* and to establish a definitive diagnosis of XL-HED (subject #23 was previously confirmed for XL-HED). Both previously reported and novel mutations were identified (eTable SII—see Supporting information online). Mutations were comprised mainly of missense mutations (n = 9; 75%), and affected the TNF (n = 5; 42%), furin (n = 3; 25%), transmembrane (n = 2; 17%), collagen (n = 1; 8%), and extracellular (n = 1; 8%) domains of the EDA1 protein (eTable SII—see Supporting information online).

Age Correlation Analysis

Although the median age for subjects in both groups was approximately 25 years, 5/12 XL-HED subjects were under 18 years of age compared with none of the controls. Given that XL-HED subjects tended to be younger than the controls, we wanted to ensure that differences in hair properties between both groups were not due to differences in age. To analyze this, we conducted a Pearson correlation analysis comparing age with the ratio of terminal to vellus hairs, the percentage of terminal hairs in anagen, and the number of FUs per cm^2 (eFig. S1—see Supporting information online). Age did not correlate with the differences we found in hair and FU properties between groups.

DISCUSSION

To develop treatments for XL-HED, it is critical that the medical genetics community identify and fully characterize the XL-HED-associated phenotypes targeted for intervention. The non-invasive collection of reproducible, quantifiable, and specific parameters will aid in the assessment of treatment efficacy. In this study, we used novel applications of non-invasive methods to precisely quantify sweat duct hypoplasia and sparse hair phenotypes, traits that significantly affect the daily lives of individuals with XL-HED.

A major morbidity associated with XL-HED is heat intolerance due to hypoplastic or absent sweat glands. Our study, similar to others [Schneider et al., 2011], found that all XL-HED subjects reported heat intolerance, a trait that limited their ability to exercise and participate in outdoor activities. It also influenced their choice of career, place to live, and travel destinations. Previous studies have utilized methods such as graphite prints [Schneider et al., 2011] and impressions of the fingertips with light body impression material [Clarke et al., 1987] to measure sweat ducts. However, these methods are not sensitive or readily reproducible. Another study used punch biopsies of the palm or scalp [Rouse et al., 2004] to analyze all sweat gland structures. Although more sensitive at detecting sweat glands and ducts, this technique is highly invasive. Our method of using confocal imaging of the palm to measure sweat ducts is sensitive, reproducible, and non-invasive. We determined that XL-HED subjects presented with few or no sweat ducts compared to controls. We noted that all XL-HED subjects showed a complete absence of sweat determined using pilocarpine iontophoresis, a standard, inexpensive, and non-invasive method to measure sweat production [Schneider et al., 2011]. These data confirm that individuals with XL-HED lack normally functioning sweat ducts and glands, and further support the role of the *EDA1* gene in the formation of sweat ducts and glands during early development [Cui and Schlessinger, 2006; Cui et al., 2008].

This study is the first to use phototrichogram analysis to quantify the hair phenotype of XL-HED subjects. Overall, we found that the thin hair phenotype observed in XL-HED subjects was due to multiple factors such as fewer terminal hairs with decreased thickness and slower growth rate, fewer FUs, and fewer hairs per FU. Interestingly, the percentage of terminal hairs in anagen did not differ between control and XL-HED groups. This observation suggests that a different mechanism is involved in the XL-HED-associated hair phenotype compared to androgenetic alopecia (i.e., male or female pattern baldness), where a decreased percentage of hairs in anagen has been reported, and drug therapies have been developed such as finasteride that target the anagen phase [Van Neste et al., 2000; Boyapati and Sinclair, 2012]. However, therapies that may be effective in XL-HED may also offer new approaches to treating androgenetic alopecia and other disorders of hair loss such

as targeting hair thickness, number of FUs, and number of hairs per FU.

To date, clear correlations between genotype and phenotype have not been determined in XL-HED. We attempted to identify genotype–phenotype correlations using regression analysis to determine relationships between the type of mutation (missense, nonsense, or deletion) or the region of EDA1 affected (TNF, furin, transmembrane, collagen, or extracellular domains) with the various parameters of the sweat duct and hair phenotypes. Our analysis did not reveal any clear genotype–phenotype correlations, primarily attributable to the small sample size. Interestingly, we did observe several XL-HED individuals with unique phenotypes that may further reveal the roles that distinct EDA1 domains play in hair and sweat gland development. XL-HED subject #8, the only subject with an in-frame deletion of 36 base pairs within the collagen domain of *EDA1*, presented with hypomorphic phenotypic features that were quite different from the other XL-HED subjects. These included the presence of residual sweat ducts in conjunction with completely nonfunctional sweat glands, and hair characteristics that were similar to control subjects in hair numbers (i.e., total hairs, total anagen hairs, FUs, and hairs per FU), but abnormal in hair width and growth rate. These data suggest that the type of mutation and the protein domain(s) affected in *EDA1* may modulate the severity of the XL-HED phenotype. In contrast, XL-HED-affected brothers #5 and #6, who both harbored the same missense mutation in the furin cleavage domain of EDA, differed markedly from one another in hair number, percentage of terminal hairs in anagen, FU number, and rate of hair growth. However, the brothers possessed similar hair widths and hairs per FU. These results suggest that in addition to the type and location of mutations in the *EDA1* gene, other genetic and/or environmental factors may play a role in modulating various aspects of the XL-HED phenotype.

Recently, an XL-HED family was described with a highly variable clinical phenotype, and it was found that some family members carried a mutation in *EDAR* (370A) that attenuated the phenotype [Cluzeau et al., 2012]. Thus, differences in the XL-HED phenotype may also be due to additional mutations in the same pathway. Genotyping other genes involved in the ectodysplasin pathway was not part of the scope of this study; however, it will be important to determine other genetic variants in future studies. Further genetic testing in conjunction with the application of our highly quantitative methods to larger XL-HED cohorts may help to identify genotype–phenotype correlations. Although a great deal is known about the role of EDA in the development of ectodermal appendages [Mikkola and Thesleff, 2003], genotype–phenotype correlations could further our understanding of the mechanism by which EDA initiates and maintains hair follicles and sweat glands.

Our study establishes highly quantitative, reproducible, and non-invasive measures to determine hair and sweat duct phenotypes associated with XL-HED, a prerequisite for the assessment of therapies in the treatment of XL-HED.

ACKNOWLEDGMENTS

The authors would like to thank all of the participants in this study, their families, and the National Foundation for Ectodermal Dysplasias. The authors are funded in part by fellowships and grants from the National Institutes of Health (F30-DE022509 to K.B.J., F30-DE022205 to A.F.G., K99-DE022059 to A.H.J., and R01-DE021420 to O.D.K.).

REFERENCES

Blüschke G, Nüsken K-D, Schneider H. 2010. Prevalence and prevention of severe complications of hypohidrotic ectodermal dysplasia in infancy. Early Hum Dev 86:397–399.

Boyapati A, Sinclair R. 2012. Combination therapy with finasteride and low-dose dutasteride in the treatment of androgenetic alopecia. Australas J Dermatol 54:49–51.

Canfield D. 1996. Photographic documentation of hair growth in androgenetic alopecia. Dermatol Clin 14:713–721.

Casal ML, Scheidt JL, Rhodes JL, Henthorn PS, Werner P. 2005. Mutation identification in a canine model of X-linked ectodermal dysplasia. Mamm Genome 16:524–531.

Casal ML, Lewis JR, Mauldin EA, Tardivel A, Ingold K, Favre M, Paradies F, Demotz S, Gaide O, Schneider P. 2007. Significant correction of disease after postnatal administration of recombinant ectodysplasin A in canine X-linked ectodermal dysplasia. Am J Hum Genet 81:1050–1056.

Clarke A, Phillips DI, Brown R, Harper PS. 1987. Clinical aspects of X-linked hypohidrotic ectodermal dysplasia. Arch Dis Child 62:989–996.

Clauss F, Manière MC, Obry F, Waltmann E, Hadj-Rabia S, Bodemer C, Alembik Y, Lesot H, Schmittbuhl M. 2008. Dento-craniofacial phenotypes and underlying molecular mechanisms in hypohidrotic ectodermal dysplasia (HED): A review. J Dent Res 87:1089–1099.

Cluzeau C, Hadj-Rabia S, Bal E, Clauss F, Munnich A, Bodemer C, Headon D, Smahi A. 2012. The EDAR370A allele attenuates the severity of hypohidrotic ectodermal dysplasia caused by EDA gene mutation. Br J Dermatol 166:678–681.

Courtney J-M, Blackburn J, Sharpe PT. 2005. The ectodysplasin and NFκB signalling pathways in odontogenesis. Arch Oral Biol 50:159–163.

Cui C-Y, Schlessinger D. 2006. EDA signaling and skin appendage development. Cell Cycle 5:2477–2483.

Cui C-Y, Kunisada M, Esibizione D, Douglass EG, Schlessinger D. 2008. Analysis of the temporal requirement for Eda in hair and sweat gland development. J Invest Dermatol 129:984–993.

Fujimoto A, Kimura R, Ohashi J, Omi K, Yuliwulandari R, Batubara L, Mustofa MS, Samakkarn U, Settheetham-Ishida W, Ishida T, Morishita Y, Furusawa T, Nakazawa M, Ohtsuka R, Tokunaga K. 2007. A scan for genetic determinants of human hair morphology: EDAR is associated with Asian hair thickness. Hum Mol Genet 17:835–843.

Gaide O, Schneider P. 2003. Permanent correction of an inherited ectodermal dysplasia with recombinant EDA. Nat Med 9:614–618.

Hammersen JE, Neukam V, Nüsken K-D, Schneider H. 2011. Systematic evaluation of exertional hyperthermia in children and adolescents with hypohidrotic ectodermal dysplasia: An observational study. Pediatr Res 70:297–301.

Mauldin EA, Gaide O, Schneider P, Casal ML. 2009. Neonatal treatment with recombinant ectodysplasin prevents respiratory disease in dogs with X-linked ectodermal dysplasia. Am J Med Genet Part A 149A:2045–2049.

Mikkola ML. 2009. Molecular aspects of hypohidrotic ectodermal dysplasia. Am J Med Genet Part A 149A:2031–2036.

Mikkola ML, Thesleff I. 2003. Ectodysplasin signaling in development. Cytokine Growth Factor Rev 14:211–224.

Mortier K, Wackens G. 2004. Ectodermal dysplasia anhidrotic. Orphanet Encyclopedia. http://www.orpha.net/data/patho/GB/uk-ectodermal-dysplasia-anhidrotic.pdf

Mou C, Thomason HA, Willan PM, Clowes C, Harris WE, Drew CF, Dixon J, Dixon MJ, Headon DJ. 2008. Enhanced ectodysplasin-A receptor (EDAR) signaling alters multiple fiber characteristics to produce the East Asian hair form. Hum Mutat 29:1405–1411.

Nguyen-Nielsen M, Skovbo S, Svaneby D, Pedersen L, Fryzek J. 2013. The prevalence of X-linked hypohidrotic ectodermal dysplasia (XLHED) in Denmark, 1995–2010. Eur J Med Genet DOI: 10.1016/j.ejmg.2013.01.012 [Published online ahead of print February 14, 2013].

Rajadhyaksha M, González S, Zavislan JM, Anderson RR, Webb RH. 1999. In vivo confocal scanning laser microscopy of human skin II: Advances in instrumentation and comparison with histology. J Invest Dermatol 113:293–303.

Rouse C, Siegfried E, Breer W, Nahass G. 2004. Hair and sweat glands in families with hypohidrotic ectodermal dysplasia: Further characterization. Arch Dermatol 140:850–855.

Schneider H, Hammer NJ, Preisler-Adams S, Huttner K, Rascher W, Bohring A. 2011. Sweating ability and genotype in individuals with X-linked hypohidrotic ectodermal dysplasia. J Med Genet 48:426–432.

Sinclair RD, Dawber RP. 2001. Androgenetic alopecia in men and women. Clin Dermatol 19:167–178.

Stenn KS, Paus R. 2001. Controls of hair follicle cycling. Physiol Rev 81:449–494.

Van Neste D, Fuh V, Sanchez-Pedreno P, Lopez-Bran E, Wolff H, Whiting D, Roberts J, Kopera D, Stene JJ, Calvieri S, Tosti A, Prens E, Guarrera M, Kanojia P, He W, Kaufman KD. 2000. Finasteride increases anagen hair in men with androgenetic alopecia. Br J Dermatol 143:804–810.

Zhang Y, Tomann P, Andl T, Gallant NM, Huelsken J, Jerchow B, Birchmeier W, Paus R, Piccolo S, Mikkola ML, Morrisey EE, Overbeek PA, Scheidereit C, Millar SE, Schmidt-Ullrich R. 2009. Reciprocal requirements for EDA/EDAR/NF-κB and Wnt/β-Catenin signaling pathways in hair follicle induction. Dev Cell 17:49–61.